

SUPPLEMENTARY MATERIALS

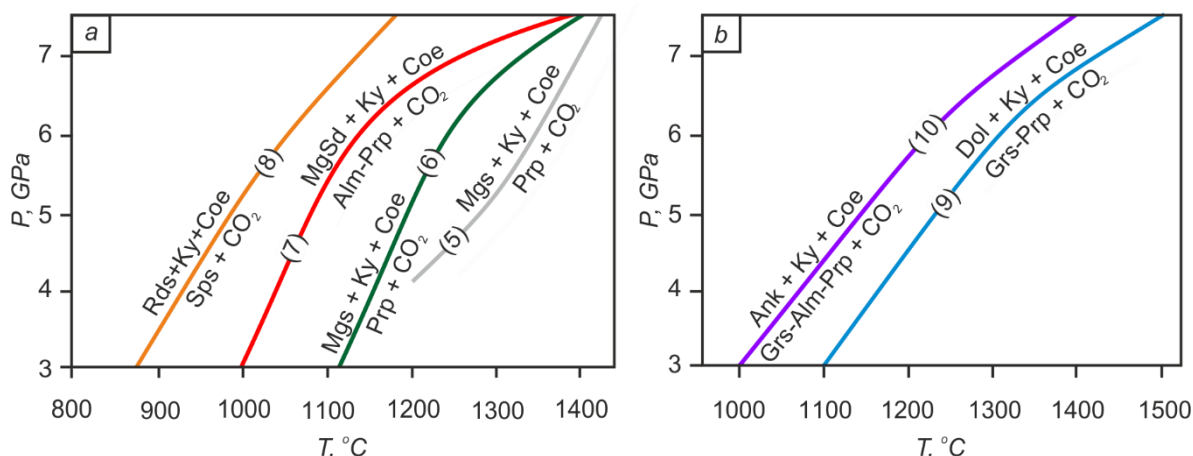
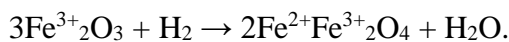


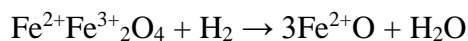
Fig. 1s. Decarbonation parameters of calcite (a) and dolomite (b) group minerals involving formation of garnets [Knoche et al., 1999; Bataleva et al, 2020a, b, c]. Ky – kyanite, Coe – coesite, Rds – rhodochrosite, Sps – spessartine, MgSd – Mg-bearing siderite, Alm – almandine, Mgs – magnesite, Prp – pyrope, Grs – grossular, Ank – ankerite, Dol – dolomite.

Calibration details. Pressure was calibrated at room temperature by the change in the resistance of Bi at 2.55 GPa, and of PbSe at 4.0 and 6.8 GPa, and at high temperatures by the graphite-diamond equilibrium (Kennedy and Kennedy, 1976). Even though pressure was not measured directly in the temperature interval of 950-1450 °C it can be roughly estimated using the result of apparatus calibration by melting of aluminium and silver at 6.3 GPa. Melting temperatures of said metals depend on pressure. Deviation of measured Al and Ag melting temperatures from established for 6.3 GPa ПIIa [Wirwald, Kennedy, 1979; Lees, Williamson, 1965] are 20-30 °C and lie within the measurement error. This way it can be concluded that the real pressure of experiment is maximally close to that calculated based on calibrations described above.

Hematite buffering container. Phase composition of the buffering container analyses were carried out after the experiments. After experiments in temperature range of 950-1350 °C composition of the container was represented by hematite and magnetite, and in temperature range of 1450-1550 °C magnetite and wüstite were identified. The main objective of using the buffering container is to maintain low f_{H_2} , which is achieved due to hydrogen oxidation according to reaction:



This way, oxygen fugacity stays close to MH (magnetite/hematite) level, and that, in its turn, provides low hydrogen fugacity and low H₂O concentration in Pt ampoules [Palyanov et al., 2010]. In the course of the experiment, the quantity of hematite in the container is decreasing while the quantity of magnetite is increasing. That can lead to appearance of monomineralic magnetite sites where magnetite reduction is possible:



This reduction causes oxygen fugacity to drop down to WM (wüstite/magnetite) equilibrium buffer level, especially on the final stages of the experiments. At the temperatures higher than 1350 °C (P = 6.3 GPa) WM buffer equilibrium provide f_{O_2} values greater than for CCO buffer (fig. 2). Such values of oxygen fugacity also maintain low f_{H_2} and H₂O concentration in Pt ampoules, as

it was established in experiments in $\text{MgCO}_3\text{-Al}_2\text{O}_3\text{-SiO}_2$ system. Fluid recovered after these experiments was analyzed using mass-spectrometry, and its composition was found to be CO_2 without H_2O impurities. The said above was true for all the experiments, including those in which wüstite presence in buffering container was determined [Bataleva et al., 2020a]. Summarizing the information given above it can be concluded that the hematite buffering container is an effective tool for control of fluid composition in petrological experiments with CO_2 involved.

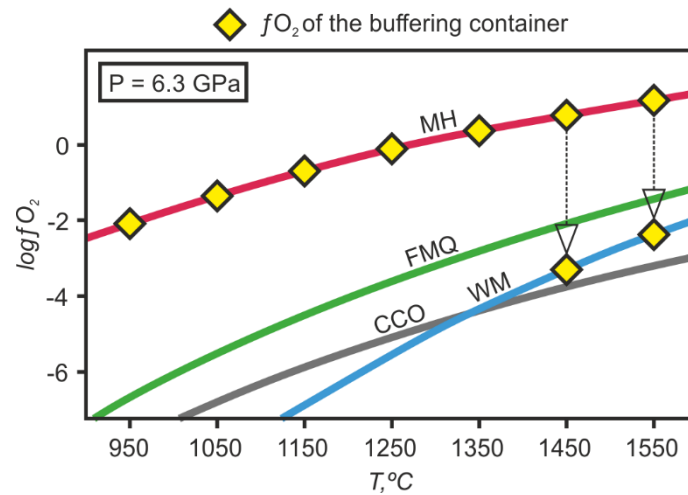


Fig. 2s. Diagram with buffer equilibria in T- $\log f\text{O}_2$ coordinates. MH – magnetite/hematite, FMQ – fayalite/magnetite+quartz, CCO – C/CO, WM – wüstite/magnetite. [Kadik, Lukanin, 1986; Ballhaus et al., 1991; Frost, Wood, 1997].

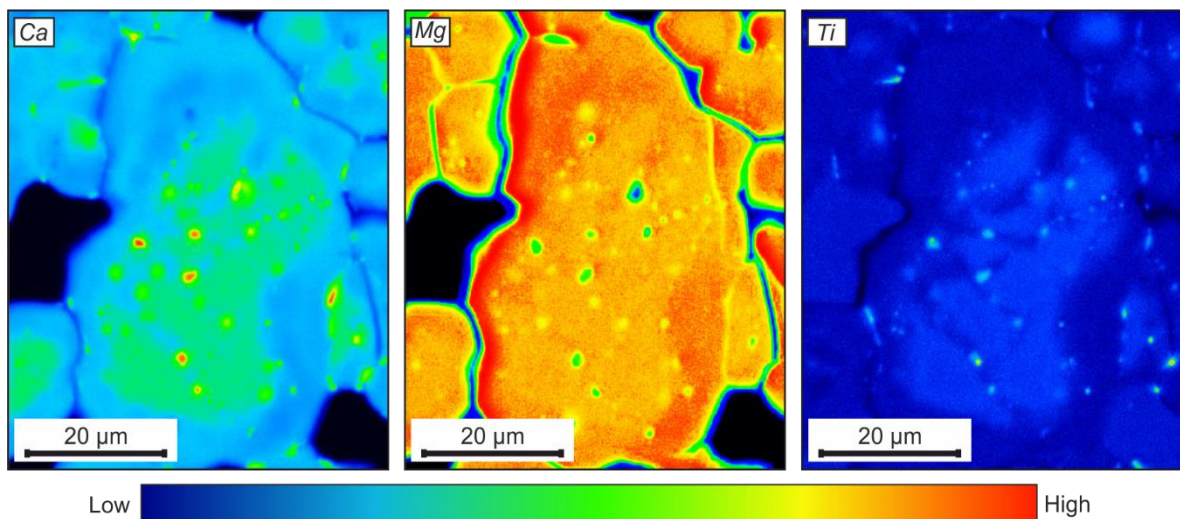


Fig. 3s. Elemental maps of garnet from experiment in $\text{Grt}_{\text{EC}}\text{-CO}_2\text{-C}$ system at 1450 °C.

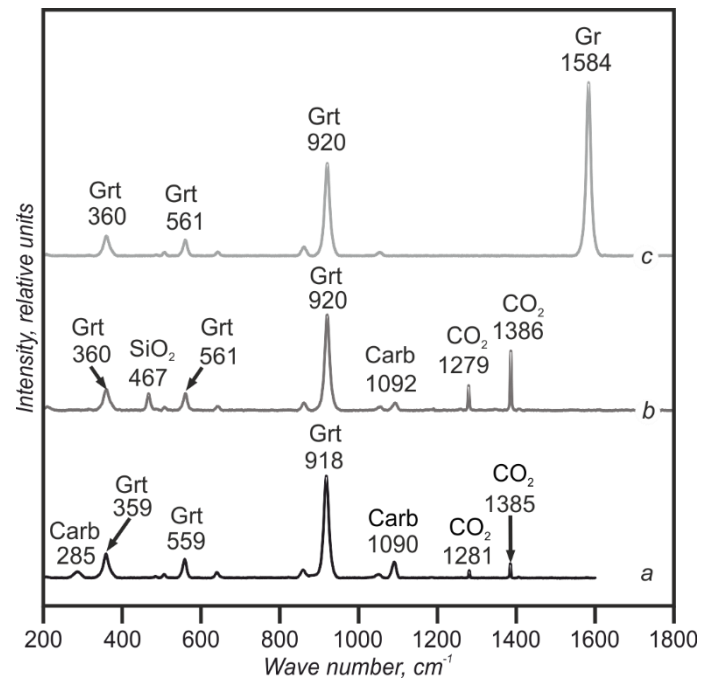


Fig. 4s. Raman spectra of inclusions in garnet crystals from experiments in Grt_{EC}-CO₂-C system at 1450 °C (a), and 1550 °C (b,c). Gr – graphite, Grt – garnet, Carb - carbonate.

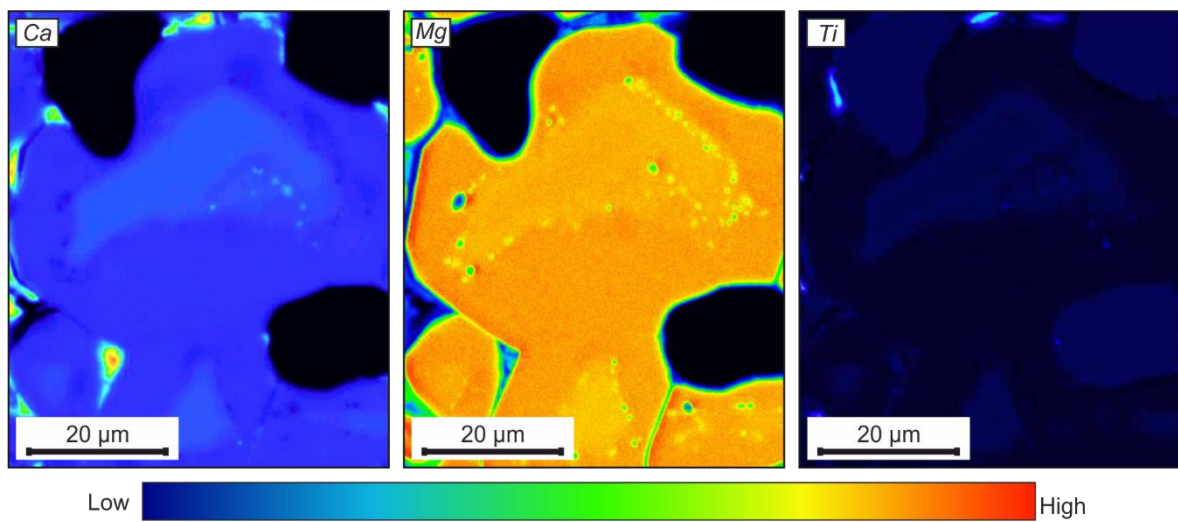


Fig. 5s. Elemental maps of garnet from experiment in Grt_{LZ}-CO₂-C system at 1450 °C.

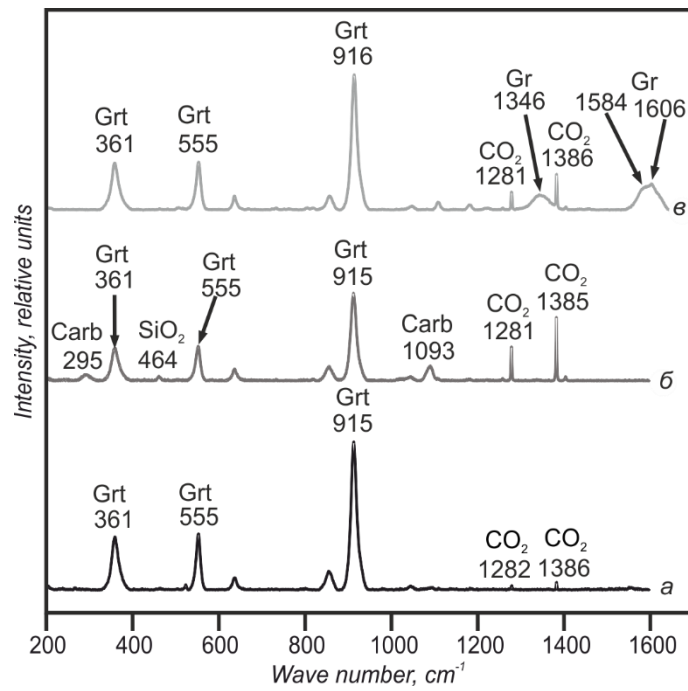


Fig. 6s. Raman spectra of inclusions in garnet crystals from experiments in Grt_{LZ}-CO₂-C system at 1350 °C (a), 1450 °C (b), and 1550 °C (c). Gr – graphite, Grt – garnet, Carb - carbonate.

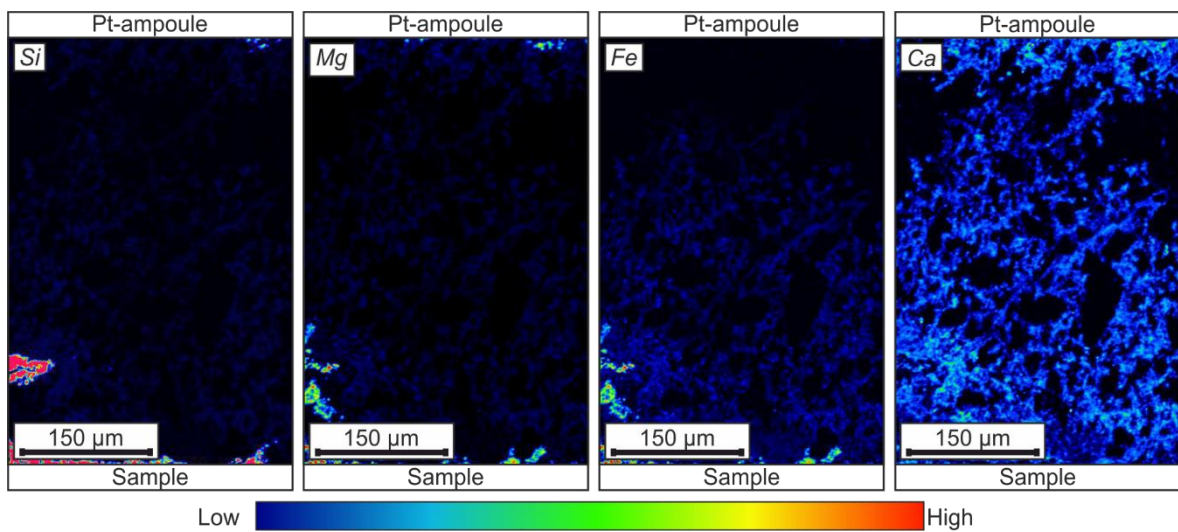


Fig. 7s. Elemental maps of the graphite capsule from experiment in Grt_{LZ}-CO₂-C system at 1250 °C (duration of 60 hours).

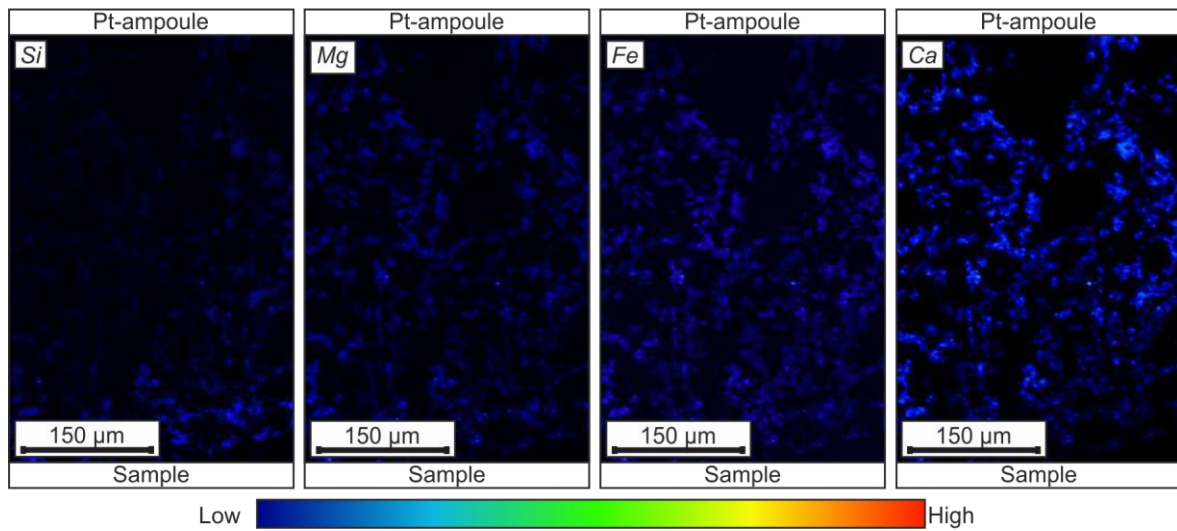


Fig. 8s. Elemental maps of the graphite capsule from experiment in Grt_{EC}-CO₂-C system at 1550 °C (duration of 5 hours).

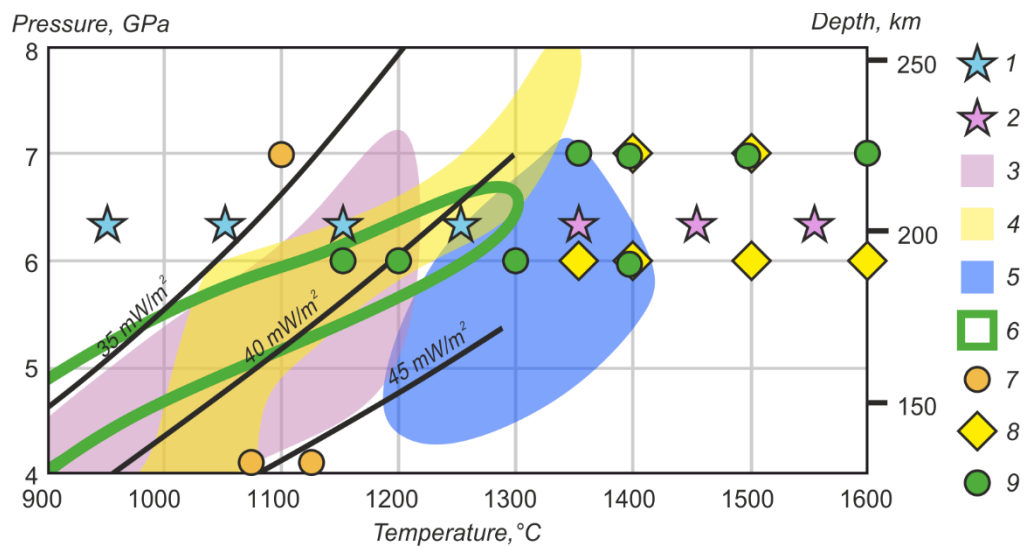


Fig. 9s. P,T-parameters of the performed experiments (1,2) and some experiments in carbonated eclogites (7) [Dasgupta et al., 2004] and carbonated peridotites (8, 9) [Brey et al., 2008; Stagno, Frost, 2010], as well as estimates for equilibration of xenoliths of North American pyroxenites and peridotites (6) [Kopylova et al., 1999], of xenolith of Slave craton (3) and Udachyana pipe (4) eclogites and of eclogitic inclusions in diamonds from Premier pipe (5) [Simakov et al., 2008]; mantle geotherms for heat flow of 35, 40, and 45 mW/m² after [Pollack and Chapman, 1977].